Angle-resolved photoemission study of the (100) surface of substoichiometric TiN: A vacancy-induced state

P. A. P. Lindberg, L. I. Johansson, and J. B. Lindström
Department of Physics and Measurement Technology, Linköping University, S-581 83 Linköping, Sweden

D. S. L. Law
Science and Engineering Research Council, Daresbury Laboratory, Daresbury Warrington WA4 4AD, United Kingdom
(Received 19 November 1986)

The (100) surface of substoichiometric TiN has been studied in normal emission utilizing synchrotron radiation for photon energies above 27 eV. In order to interpret the spectral features in the experimental data, comparisons with band-structure results and theoretical photoemission spectra calculated for stoichiometric composition are made. A nondispersive structure is observed at about 2-eV binding energy in the recorded spectra and is interpreted as a vacancy-induced state. Its intensity variation with photon energy has been studied and is compared with a resonant enhancement of the emission from states close to the Fermi energy for photon energies between 39 and 51 eV.

I. INTRODUCTION

During the last few years, there has been much activity concerning the vacancies in the transition-metal carbides and nitrides, both experimentally and theoretically. This has been stimulated by the fact that these compounds tend to crystallize in substoichiometric phases, but do exist over a wide range of compositions. Moreover, the occurrence of vacancies in the nonmetal sublattice modifies the interesting combination of properties that this group of materials exhibits.[1] Their ultrahardness and high melting point differ significantly from those of the metal constituent, which makes them well suited as coatings for wear-resistant materials. They have high electrical conductivity and some of them are among the best superconductors known today. A further investigation of the defect structure and its consequences on the electronic structure—a structure that essentially determines the macroscopic properties of a material—seems therefore to be well motivated.

Vacancy-induced effects have been observed in both theoretical[2–5] and experimental[6–10] studies on substoichiometric carbides and nitrides of transition metals. A peak at 2-eV binding energy has been observed in angle-integrated photoemission experiments on polycrystalline samples of TiN,[7,9,10] ZrN,[6,9,10] and NbC.[8] The intensity of this peak was shown to increase with the vacancy concentration, and it could not be explained on the basis of a stoichiometric electronic structure. Since theoretical models have confirmed these results by predicting the creation of new filled states at about 2 eV below the Fermi energy, there seems to be no doubt about the origin of the feature observed in angle-integrated photoemission studies on nonmetal-deficient samples of these compounds.

However, no angle-resolved study of the vacancy-induced structure has been reported, and surface segregation effects, which would allow for a different vacancy concentration at the surface, have not been examined experimentally. The latter would lead to a surface vacancy concentration that is not representative of the bulk, and therefore surface-sensitive techniques such as ultraviolet photoemission spectroscopy (UPS) would give misleading information about the bulk properties. It has been argued on rather vague grounds that high-temperature treatments, such as flash heatings, would totally destroy the presence of vacancies at the surface and thus produce a pure stoichiometric surface. Recent theoretical results[2,3] have shown that for substoichiometric TiN, a vacancy-induced structure would be visible in normal photoemission from the (100) surface at excitation energies above 36 eV. So far, angle-resolved photoemission experiments on single-crystal TiN have been performed with conventional discharge lamps using He I and Ne I radiation and synchrotron radiation up to 33 eV.[11] No vacancy-related structure was observed, however, in those experimental spectra.

It is the aim of the present work to complete the earlier angle-resolved studies by utilizing synchrotron radiation at higher energies in normal emission experiments, thus making a direct comparison with recent theoretical results on substoichiometric TiN feasible. Normal photoemission spectra for photon energies in the range 29 to 63 eV are presented and also compared with calculated spectra[12] for stoichiometric composition. The origin and symmetry of the observed peaks are discussed and a comparison with band-structure calculations is made. The experimental spectra are presented in relative units in order to follow a resonant enhancement of the electron emission from states located just below the Fermi energy. A vacancy-induced state is observed at around 2 eV below the Fermi level and its connection to the resonance mentioned above is discussed.

II. EXPERIMENT AND COMPUTATION

A. Experimental procedure

Angle-resolved photoemission experiments were carried out at station 6.2 at the Daresbury Synchrotron Radiation

Source. This beam line is equipped with a toroidal grating monochromator and a Vacuum Generators ADES 400 photoemission system. The hemispherical electron analyzer had an acceptance cone of $\pm 2°$, and the energy resolution of the monochromator and analyzer were generally chosen to be 0.18 and 0.20 eV, respectively, which gave a total energy resolution of less than 0.3 eV. The experiments were performed at a base pressure of less than 1×10^{-10} torr. A tungsten grid mounted in front of the photoemission system allowed for photon flux normalization by recording the electron yield from the grid for each photoemission spectrum.

The preparation of the crystal used in the experiments has been described previously.[13] The crystal was mounted with the (100) surface perpendicular to the analyzer plane within $\pm 1°$. It was cleaned *in situ* by repeated flash heatings to about 1600 °C, which was found to give a clean surface for about 6 h. The crystal was oriented using low-energy electron diffraction (LEED) and a clear 1×1 LEED pattern was observed without any sign of contamination. Prior to measurement, the cleanliness of the sample was checked using UPS and no residual oxygen was detected. In the experimental spectra presented below, the emission angle of the electrons, θ_e, and the angle of incidence of the radiation, θ_i, are given relative to the sample surface normal. In all spectra presented below, the midpoint of the Fermi edge has been used as a reference point.

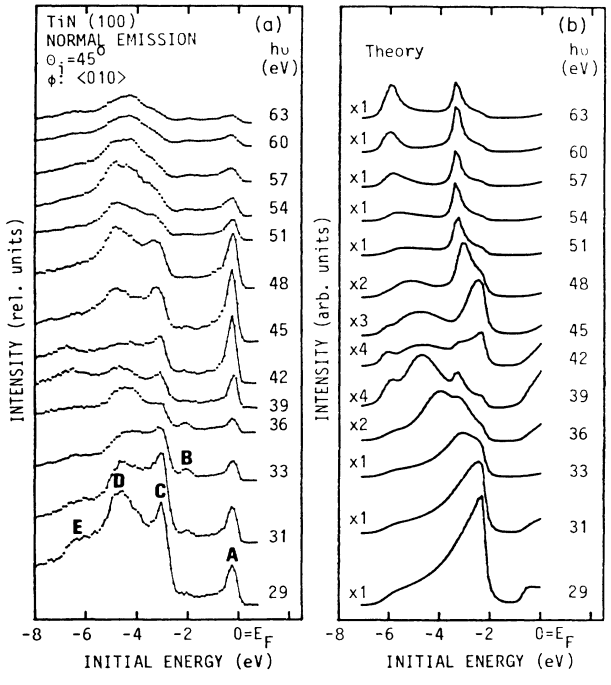

FIG. 1. (a) Experimental angle-resolved normal-emission energy distribution curves for TiN(100). The radiation is incident along the ⟨010⟩ azimuth and at an incidence angle $\theta_i=45°$ with respect to the surface normal. (b) Calculated spectra to be compared with the experimental results in (a).

B. Computational details

In an earlier work,[14] photoemission spectra from the TiN(100) surface were calculated and compared with experimental results for normal as well as off-normal electron emission. These calculations were based on the extended version of the time-reversed LEED theory scheme.[15] Since the overall agreement between the experimental and theoretical spectra was found to be very good, the same theoretical approach has been chosen in the present work. This means that a surface overlayer was introduced, in which the potential at the nitrogen atoms was shifted relative to that of the bulk by $+0.4$ eV. The bulk potential was the same as the one generated in a linearized augmented plane-wave (LAPW) band-structure calculation on stoichiometric TiN.[11] This choice of potential for surface and bulk is motivated by its success in accounting for a Tamm surface state on TiN, as has been reported in previous work.[12,14] The surface layer has been assumed to be nondistorted, and bulk lattice parameters have been used also for the top layer. The lifetime-broadening parameters were chosen to be 2.0 and 0.14 eV for the high- and low-energy electronic states, respectively, and 21 reciprocal lattice vectors were used in the calculations to insure convergence. The polarization of the incident radiation has been chosen to be purely linear in the plane of incidence. No corrections for refraction and reflection of the incident radiation at the surface have been done.

III. RESULTS AND DISCUSSION

A. Interpretation of photoemission spectra

Experimental angle-resolved energy distribution curves (EDC's), for photon energies between 29 and 63 eV, are shown in Fig. 1(a). The spectra were recorded at normal emission, and the radiation was incident along the ⟨010⟩ azimuth at an angle of $\theta_i=45°$. The ECD's have been normalized so that the evolution of the peak intensities with photon energy can be followed. To obtain the normalization of these spectra, the variation of the incident flux was recorded and constant-initial-state measurements were also performed. Five structures are observed in the spectra. The peak labeled *A* in Fig. 1(a), located just below the Fermi energy, exhibits a strong dependence on photon energy. The intensity of this peak is seen to change dramatically for photon energies in the region 39–51 eV. The emission from peak *B*, which shows little or no dispersion with photon energy, is also strongly affected by the energy of the incident radiation. It exhibits a strength that goes through a maximum at 33 eV, but is also clearly visible at higher energies. The three lowest-lying structures, labeled *C*, *D*, and *E*, are easily discernible at lower energies, and exhibit little dispersion with photon energy.

The corresponding calculated spectra are shown in Fig. 1(b). The overall agreement between the experimental and theoretical spectra for peaks *C*, *D*, and *E* is found to be fairly good. The dispersion and relative intensity are, in general, well reproduced by the theoretical curves. Especially at intermediate photon energies, around 39 eV,

the energy position as well as peak width are very well mimicked by the calculations. However, there are also some features in the experimental EDC's that are not so well reflected by the calculated spectra. The calculations cannot explain peak B and the intensity modulations of peak A in the experimental spectra. The intensity variation of peak A can partly be explained by the calculated curves for photon energies below 33 eV, but at higher energies there is a severe discrepancy. Peak B seems to have no counterpart in the calculated curves, since there is no feature in the calculated spectra that can account for its nondispersive character and photon energy dependence. These discrepancies are not accidental as will be explained in later sections. Furthermore, the theoretical features are in general narrower and exhibit, at some photon energies, a shoulder, located at about -2.3 eV, that cannot be observed in the experimental EDC's. These discrepancies could be due to the nonideal experimental situation, which broadens the spectral features considerably, especially at higher photon energies. The calculations assume a monochromatic excitation source, a perfectly smooth sample surface, and a vanishingly narrow acceptance cone of the analyzer. These are all idealizations that can never be fulfilled under experimental conditions. Moreover, the lifetime-broadening parameters, which determine the width of the calculated structures, have not been optimized to reproduce the experimental results. It is also noted that at higher photon energies the lowest-lying structure is more pronounced in the calculated spectra. This difference between the experimental and calculated spectra might be due to the fact that at higher photon energies a larger region of the Brillouin zone is probed by the analyzer, while the calculations still assume that only electrons leaving the crystal with zero momentum parallel to the sample surface can contribute to the photoemission current. It should also be kept in mind that the degree of polarization of the radiation is lower at the higher photon energies.[16] The experimental and calculated spectra for a smaller incidence angle, $\theta_i = 18°$, are shown in Figs. 2(a) and 2(b), respectively. Again, the experimental EDC's are presented in relative units to allow for observation of peak intensity variations. Concentrating first on the experimental spectra, we note that some significant changes have occurred by decreasing the incidence angle from $\theta_i = 45°$ to $\theta_i = 18°$. Peaks B, D, and E, observed in Fig. 1(a), have almost disappeared, and peak C has gained relative intensity. We note that peak A still exhibits a resonant behavior in the energy range 39–51 eV, but has gained relative strength for photon energies below 33 eV, as compared with the larger incidence angle. The corresponding intensity changes in the theoretical spectra are in accordance with the experimental findings; the two lowest-lying structures have become considerably weaker and are now hardly visible in the spectra. Moreover, the emission from the peak just below the Fermi energy has increased markedly at lower photon energies and reproduces the intensity variation of peak A fairly well for photon energies below 33 eV. However, the calculated curves cannot explain the resonant enhancement of this peak at intermediate energies, as was already noted for $\theta_i = 45°$. The dispersion of peak C is reflected quite well by the calculations, although, at lower photon energies, the theoretical results locate its energy position about 0.6 eV closer to the Fermi energy. As in the case of $\theta_i = 45°$, the calculated structures are generally sharper and exhibit, at higher photon energies, a shoulder that is not discernible in the experimental spectra. These discrepancies are most pronounced at higher photon energies, where the difference between the experimental and theoretical approach is largest, as was already discussed for the larger incidence angle.

So far, we have not tried to explain the origin of the experimental features. We have seen that the calculated spectra satisfactorily reproduce the three lowest-lying experimental structures. Since the calculated curves are based on stoichiometric TiN, one might therefore be led to interpret peaks C, D, and E as originating from bulk energy bands of TiN. In order to see if this is the case, a comparison with band-structure calculations has to be made. This comparison is facilitated considerably by referring to group-theoretical results.[17,18] It is well known that at normal emission from the (100) surface of a crystal with fcc symmetry, only the final states of Δ_1 symmetry contribute to the photoemission current. In the dipole approximation, this implies that the only allowed electronic transition is $\Delta_5 \rightarrow \Delta_1$ ($\Delta_1 \rightarrow \Delta_1$) when the electric field vector is parallel (perpendicular) to the surface plane. Since the normal component of the electric field increases monotonically with increasing incidence angle, photoemission peaks originating from bands of Δ_1 symmetry should

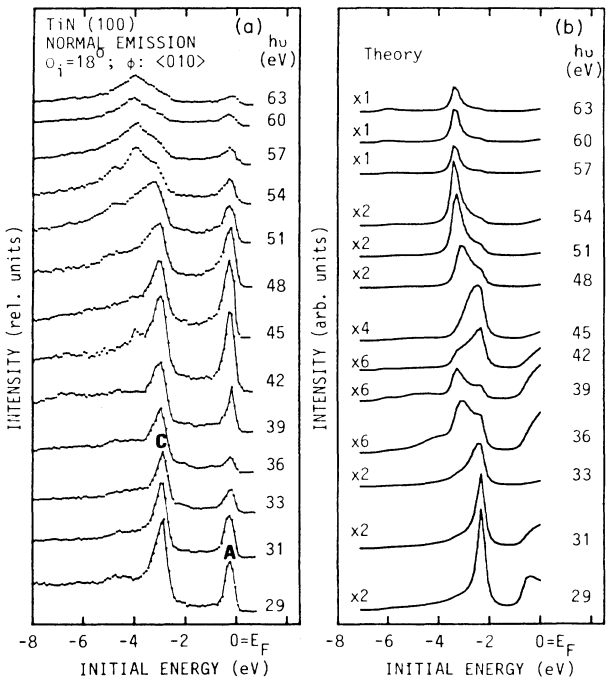

FIG. 2. (a) Experimental angle-resolved normal-emission energy distribution curves for TiN(100). The radiation is incident along the ⟨010⟩ azimuth and at an incidence angle $\theta_i = 18°$ with respect to the surface normal. (b) Calculated spectra to be compared with the experimental results in (a).

gain strength as the incidence angle becomes larger, and vice versa for states of Δ_5 symmetry. To identify the symmetry of peaks *C*, *D*, and *E*, normalized EDC's for a photon energy of 36 eV are shown in Fig. 3 for both incidence angles. It is seen from this figure that peaks *B*, *D*, and *E* show a dependence on θ_i that can be associated with transitions from states of Δ_1 symmetry. In contrast, peak *C* is seen to gain intensity by increasing the parallel component of the electric field, indicating that it originates from initial states of Δ_5 symmetry.

The dispersion of the experimental peaks for photon energies in the range 27–66 eV, along the Γ-*X* symmetry line, is shown in Fig. 4, together with a calculated band structure for stoichiometric TiN from Johansson *et al.*[11] The open circles represent the location of peak *B* and the solid circles indicate the position of the other four peaks. To determine the location of the experimental peaks, the direct-transition model has been used together with the fact that only totally symmetric final states are allowed at normal emission. Calculated final-state bands have been used for photon energies up to 42 eV, and a free-electron-like band at higher energies. An inner potential of 6.0 eV and a free-electron mass were chosen for the free-electron band, which were found to give a reasonable fit to calculated final bands. It is seen from Fig. 4 that the peak position as well as the dispersion of peak *C* can be well explained by the lowest-lying Δ_5 band, confirming its polarization dependence. Peak *D* is assumed to originate from the steep part of the Δ_1 band, which, at lower photon energies, allows direct transitions to final bands with a similar slope. To illustrate this, the final-state band for a photon energy of 29 eV is shown in Fig. 4 as a dashed line. By keeping in mind that the energy bands do have an appreciable width, we thus see that direct transitions between bands with similar slopes are allowed over a fairly large region of the Brillouin zone. This may explain why

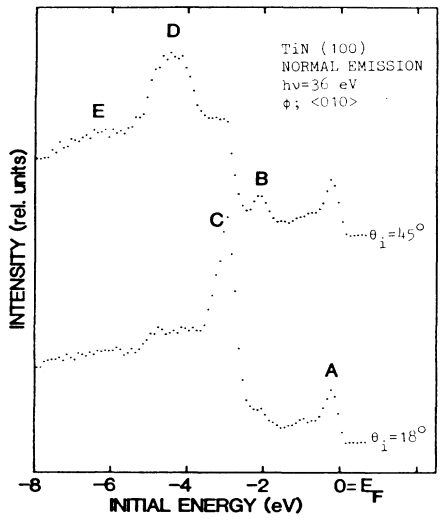

FIG. 3. Angle-resolved energy distribution curves for two angles of incidence, $\theta_i = 18°$ and 45°. The spectra were measured at normal emission for a photon energy of 36 eV.

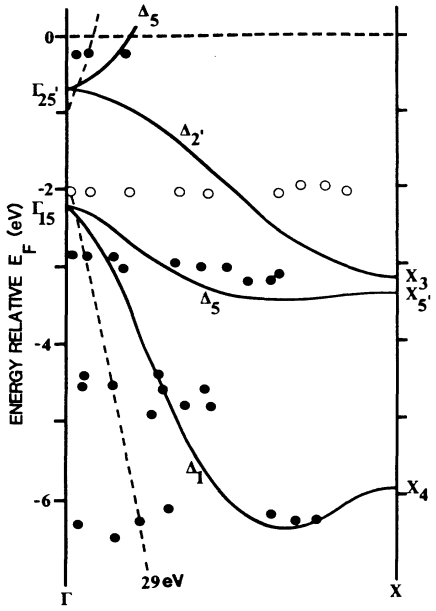

FIG. 4. Comparison between the location of the experimentally observed peaks along the Γ-*X* symmetry line and calculated energy bands. For clarity, the final-state band used at lower photon energies, represented by the dashed line, has been displaced downwards by 29 eV.

this peak shows little dispersion with photon energy and has a considerable width. In contrast, peak *E* is located close to the flat portion of the Δ_1 band, indicating that this peak might arise from one-dimensional density-of-states (DOS) effects. This interpretation is supported by the strong polarization dependence and the small dispersion with photon energy that peak *E* exhibits. It is also seen in Fig. 4 that direct transitions involving electrons occupying the uppermost Δ_5 band may contribute to the emission intensity of peak *A* at lower photon energies. This observation is consistent with the earlier comparison between the experimental and calculated spectra for the two incidence angles. There are, however, no bulk bands that can explain the behavior of peak *A* around 45 eV, which indicates that the resonant enhancement of emission from states just below the Fermi energy is due to a more complicated transition mechanism. We also note that there is no bulk band that can account for peak *B*; its nondispersive character and location in the gap between the two (symmetry-allowed) Δ_5 bands, together with its polarization dependence are taken as evidence that this peak cannot be explained on the basis of stoichiometric TiN.

Previously, it was seen that there is a severe difference between the experimental and calculated spectra at higher photon energies; the spectral widths as well as the relative intensities of the features were found to be markedly different. This observation indicates that other processes may start to dominate at these energies. At higher photon energies a large region of reciprocal space will be probed by the analyzer, mainly due to its finite acceptance

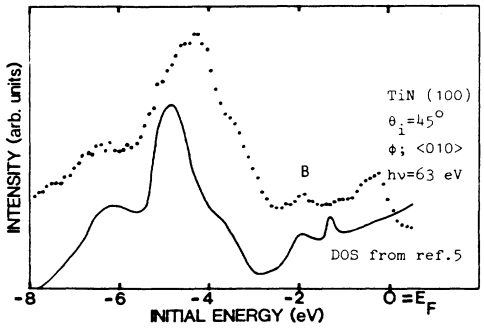

FIG. 5. Comparison between an experimental angle-resolved energy distribution curve from TiN(100) recorded using radiation of energy 63 eV, and a density-of-state (DOS) spectrum calculated for $TiN_{0.83}$ (from Ref. 5).

cone. In the limit of very high photon energies, the electronic DOS would therefore effectively be seen by the analyzer. In Fig. 5, the EDC for $h\nu=63$ eV and $\theta_i=45°$ is compared with a DOS calculation for $TiN_{0.83}$ due to Marksteiner *et al.*[5] The calculations assume completely randomly arranged vacancies, which are shown to induce a peak at about 2 eV binding energy. There is a fairly good agreement between the experimental curve and the DOS calculation; the overall shape of the experimental curve is quite well reproduced by the DOS calculation. Furthermore, Fig. 5 indicates that peak *B* may be related to the presence of vacancies in the nitrogen sublattice.

To this point, the two most significant differences between the experimental and calculated spectra—the failure of the calculations to account for (i) the resonant emission from states close to the Fermi energy and (ii) the appearance of a peak at 2 eV binding energy, showing a strong dependence on photon energy and polarization—have not been explained. These two features will therefore be treated separately in the following two sections.

B. Photon-induced resonance at the Fermi energy

To obtain a more detailed picture of the resonant enhancement of peak *A*, a constant-initial-state (CIS) measurement was performed. During the CIS measurement, the photon energy and kinetic energy of the detected electrons were scanned simultaneously, so that the intensity variation of peak *A* could be followed. In order to obtain a properly normalized CIS curve, a two-step procedure was used. The yield from the beam monitor was used as a reference counter during the measurements. The curve thus obtained was corrected for variations in the absorption efficiency of the tungsten beam-monitor grid.[19] The resulting CIS curve is represented in Fig. 6 by crosses. It is seen from this figure that peak *A* exhibits a shallow minimum at 35 eV and a pronounced but quite broad maximum centered at about 44 eV. These results are in qualitative agreement with previously reported CIS data on polycrystalline TiN,[9] although our curve shows a much sharper high-energy cutoff. Resonances of the type shown in Fig. 6 are fairly common among the transition metals and have been explained as due to transition of the form

$$3p^6 3d^2 + h\nu \rightarrow 3p^5 3d^3 \rightarrow 3p^6 3d^1 + e^- ,$$

that is, a $p \rightarrow d$ excitation followed by a super–Coster-Kronig decay. Since the DOS at the Fermi energy originates mainly from titanium $3d$ states,[5] transitions of this type would lead to resonant emission from states located at the Fermi energy. In order to examine the relationship between the resonant behavior of peak *A* and the absorption of photons, a constant-final-state (CFS) measurement was carried out. In the CFS measurement, the intensity of the inelastically scattered electrons was measured as a function of the photon energy by keeping the kinetic energy of the analyzed electrons fixed to 3 eV; thus a CFS measurement gives essentially the absorption of radiation as a function of photon energy. The CFS curve, normalized according to the procedure described above, is shown in Fig. 6 as the dotted curve. For comparison, the absorption coefficient of titanium[20] (dashed curve) is also shown. By inspecting Fig. 6 more closely, several interesting observations can be made. The CFS curve exhibits a doublet structure in the region where it has its maximum, which is not observed for titanium. The shapes of the CFS and CIS curves are almost identical in

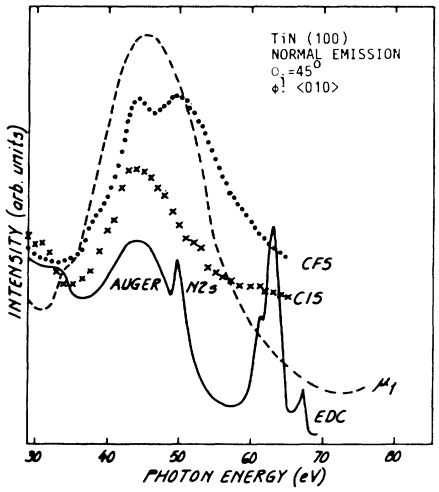

FIG. 6. Constant-initial-state (CIS) curve (crosses) showing the intensity variation of the emission from states just below the Fermi energy. The dotted curve represents the result from a constant-final-state (CFS) measurement. These two curves have been normalized with respect to variations in the incident photon flux. Also shown are the absorption coefficient curve of titanium (dashed curve) from Ref. 20 and a wide scan EDC. The EDC was recorded using 65-eV radiation incident along the ⟨010⟩ azimuth at an incidence angle of 45° with respect to the surface normal. The EDC has been displaced so that a comparison between the width of the Auger peak and the CIS curve can be made. The Auger peak is believed to be intimately related to the resonant emission from states at the Fermi energy. See text for details.

the region of the resonance onset, whereas the width of the CFS curve is considerably larger; indeed, the CIS curve seems to be intimately connected to the first peak in the CFS curve.

It is also interesting to note that the width of the CIS curve, about 10 eV, is comparable to that of an Auger peak observed at photon energies beyond the resonance region. This is also illustrated in Fig. 6, where a wide-scan EDC for a photon energy of 65 eV (solid curve) has been inserted. The Auger peak, which is believed to be due to nonresonant emission from the $3p^5 3d^3$ excited state, shows up at a fixed kinetic energy of about 37 eV. The qualitative agreement in peak width is in accordance with theoretical models[21–23] concerning this type of resonance phenomenon; the widths of the resonance in photon energy and the corresponding Auger peak are both determined by the lifetime of the created core hole.

C. Vacancy-induced effects

So far, the presence of vacancies and their contribution to the photoemission spectra have not been considered. It was seen in Sec. III A that neither the calculated spectra nor the band-structure calculation were able to explain the occurrence of a peak at 2 eV binding energy in the experimental spectra. Both these theoretical results are based on stoichiometric material, thus neglecting the presence of vacancies in the sample. One is therefore led to associate this peak as originating from occupied vacancy-related states. This interpretation is supported by recent photoemission calculations on substoichiometric TiN. Redinger *et al.*[2] showed that a vacancy-induced structure appears in normal photoemission spectra from substoichiometric TiN for photon energies above 36 eV. This peak, located at about 2 eV binding energy, was shown to have a strong dependence on both the energy and polarization of the incident radiation. The structure was clearly observed at photon energies above 36 eV and at an incidence angle of $\theta_i = 45°$, and was shown to go through a relative maximum at a photon energy of 42 eV. These theoretical results predict fairly well the behavior of our experimental spectra. The polarization dependence of this peak, shown in Fig. 3 for $h\nu = 36$ eV, indicates that this feature is most efficiently excited by the normal component of the electric field. The dependence on photon energy is illustrated in Fig. 7, where the evolution of the vacancy-induced structure with photon energy is shown for the larger incidence angle, $\theta_i = 45°$. It is seen that the peak exhibits a resonant behavior for photon energies between 29 and 36 eV, with a pronounced maximum at 33 eV. The latter observation is in qualitative agreement with the calculations from Redinger *et al.*,[2] although the theoretical spectra show a resonant enhancement at about 10-eV higher energy.

It is not clear why this feature was not observed in the earlier angle-resolved normal emission spectra using the same cleaning procedure and photon energies above 30 eV.[11] A possible explanation may be that the enhancement of contamination during a long series of measurements is able to totally conceal the vacancy structure of the material. Studies on TiC[24–26] have shown that the surface reactivity is dramatically enhanced when vacancies in the carbon sublattice are created deliberately.[26]

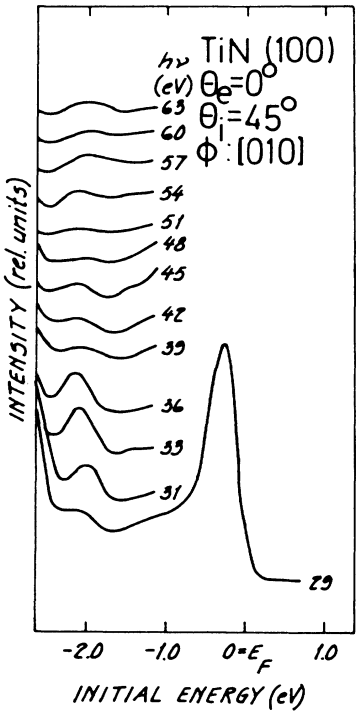

FIG. 7. The evolution of the vacancy structure with photon energy. The spectra were recorded at normal emission and at an incidence angle of 45°. The vacancy structure is located at about −2 eV relative to the Fermi edge.

In order to see if the resonances observed for the vacancy peak and the peak at the Fermi energy are related to each other, the net area under the vacancy peak has been determined from the normalized EDC's. The result is shown in Fig. 8 together with the CIS curve for the peak close to the Fermi edge. This figure demonstrates unam-

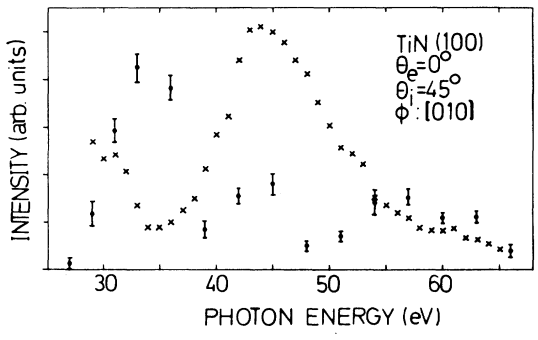

FIG. 8. Comparison between the variation of emission intensity from states just below the Fermi level (crosses) and from the vacancy structure at 2 eV binding energy (solid dots). The vertical bars are estimated uncertainties in determining the intensity of the vacancy structure. Both curves were obtained at an incidence angle of 45°. For clarity, the curve corresponding to the emission intensity of the vacancy structure has been magnified by a factor of approximately 15.

biguously that the intensity of the vacancy peak does not follow that of the resonance feature observed at the Fermi energy; in fact, the vacancy peak is most pronounced at photon energies where the CIS curve exhibits a local minimum. This observation is consistent with the partial DOS calculations by Marksteiner *et al.*,[5] which showed that the vacancy-related DOS at 2 eV below the Fermi energy has mainly *s* character, whereas the DOS at the Fermi level is dominated by the *d*-like metal partial DOS. Earlier angle-integrated photoemission measurements on TiN[9] also indicate that the vacancy state has non-*d* character. Moreover, Marksteiner *et al.*[5] have shown that the position as well as the width of the vacancy-induced partial DOS changes systematically with the vacancy concentration. Our experimental results give for the peak position and width of the vacancy peak, about -2 and 0.8 eV, respectively; in good agreement with those predicted by their calculated vacancy-induced partial DOS for $TiN_{0.83}$. Thus, the interpretation of peak *B* in the experimental EDC's as due to vacancy states is firmly supported by the theoretical results. Furthermore, since UPS is an extremely surface-sensitive technique, the impressive agreement with calculations based on a compound with the same nominal composition, indicates that the vacancy concentration at the surface seems to be about the same as in the bulk. This is particularly interesting to note, since during the last years there has been a serious questioning of the cleaning procedure used in the present work. It has been argued that flash-heatings would quench the possibility of seeing vacancy-induced effects in the UPS regime by creating a stoichiometric region at the surface. It has actually been shown on theoretical grounds[3] that one stoichiometric top layer is enough to totally conceal the vacancy-induced peak at 2 eV binding energy.

With the present results in hand, it seems very strange to us that some authors[10] have stated that it is now *known* that flash heatings lead to a stoichiometric surface layer. We believe, on the contrary, that repeated flash heatings to temperatures below about 1600 °C do not cause an appreciable vacancy concentration gradient in the surface region, and we base this on the following arguments.

(i) A vacancy-induced peak in the photoemission spectra has been identified unambiguously.

(ii) The location and width of this peak are in good agreement with DOS calculations for a compound of the same nominal composition.

(iii) No change in the vacancy peak could be observed after repeated flash heatings.

(iv) We have made similar observations on other transition-metal nitrides.

IV. SUMMARY

Synchrotron radiation for photon energies above 27 eV was used to obtain normal photoemission spectra on single-crystal $TiN_{0.83}$. Five features could be identified in the spectra, all but one exhibiting strong polarization dependence. The experimental results were compared with calculated spectra for stoichiometric TiN, which were able to reproduce the three lowest-lying structures fairly well. These structures could be interpreted as originating from bulk bands of Δ_1 and Δ_5 symmetry after comparison with band-structure calculations for stoichiometric TiN. However, the two remaining peaks in the experimental spectra, which showed a strong dependence on photon energy, could not be explained by the calculations. The pronounced resonance which the peak at the Fermi energy exhibited was shown to be consistent with transitions of the super–Coster-Kronig type and was suggested to be related to an Auger peak, observed for photon energies beyond the resonance region. The last feature was interpreted as arising from a vacancy-induced state. Its nondispersive character, polarization dependence, and location were all found to be in good agreement with theoretical results for substoichiometric TiN of the same composition. Finally, the cleaning procedure and its connection to the observed vacancy peak was discussed.

ACKNOWLEDGMENTS

The authors want to thank the staff at the Daresbury laboratory for their assistance during the experiments. This research received financial support from the Swedish Natural Science Research Council, which is gratefully acknowledged.

[1]L. E. Toth, *Transition Metal Carbides and Nitrides* (Academic, New York, 1971).
[2]J. Redinger, P. Weinberger, and A. Neckel, Phys. Rev. B **35**, 5647 (1987).
[3]J. Redinger and P. Weinberger, Phys. Rev. B **35**, 5652 (1987).
[4]G. Schadler, P. Weinberger, A. Gonis, and J. Klima, J. Phys. F **15**, 1675 (1985).
[5]P. Marksteiner, P. Weinberger, A. Neckel, R. Zeller, and P. H. Dederichs, Phys. Rev. B **33**, 812 (1986).
[6]L. Porte, Solid State Commun. **50**, 303 (1984).
[7]L. Porte, L. Roux, and J. Hanus, Phys. Rev. B **28**, 3214 (1983).
[8]H. Höchst, P. Steiner, S. Hüfner, and C. Politis, Z. Phys. B **37**, 27 (1980).
[9]R. D. Bringans and H. Höchst, Phys. Rev. B **30**, 5416 (1984).
[10]H. Höchst, R. D. Bringans, P. Steiner, and Th. Wolf, Phys. Rev. B **25**, 7183 (1982).
[11]L. I. Johansson, A Callenås, P. M. Stefan, A. N. Christensen, and K. Schwarz, Phys. Rev. B **24**, 1883 (1981).
[12]C. G. Larsson, L. I. Johansson, and A. Callenås, Solid State Commun. **49**, 727 (1984).
[13]L. I. Johansson, P. M. Stefan, M. L. Shek, and A. N. Christensen, Phys. Rev. B **22**, 1032 (1980).
[14]L. I. Johansson, C. G. Larsson, and A. Callenås, J. Phys. F **14**, 1761 (1984).
[15]J. F. L. Hopkinson, J. B. Pendry, and D. J. Titterington, Comput. Phys. Commun. **19**, 69 (1980).
[16]Experimental determinations made recently indicate a degree of polarization between about 0.6 and 0.8. D. S. L. Law (unpublished).
[17]J. Hermanson, Solid State Commun. **22**, 9 (1977).
[18]W. Eberhardt and F. J. Himpsel, Phys. Rev. B **21**, 5572 (1980).

[19]R. Haensel, K. Radler, B. Sonntag, and C. Kunz, Solid State Commun. **7**, 1495 (1969).
[20]C. Wehenkel and B. Gauthe, Phys. Lett. **47A**, 253 (1974).
[21]S. M. Girvin and D. R. Penn, Phys. Rev. B **22**, 4081 (1980).
[22]L. C. Davis and L. A. Feldkamp, Phys. Rev. Lett. **44**, 673 (1980).
[23]J. A. D. Matthew and S. M. Girvin, Phys. Rev. B **24**, 2249 (1981).
[24]C. Oshima, M. Aono, T. Tanaka, S. Kawai, S. Zaima, and Y. Shibata, Surf. Sci. **102**, 312 (1981).
[25]C. Oshima, M. Aono, S. Zaima, Y. Shibata, and S. Kawai, J. Less-Common Met. **82**, 69 (1981).
[26]M. Aono, Y. Hou, R. Souda, C. Oshima, S. Ontani, and Y. Ishizawa, Phys. Rev. Lett. **50**, 1293 (1983).